Sains Malaysiana 50(7)(2021): 1871-1884
http://doi.org/10.17576/jsm-2021-5007-04

Geophysical Characterization of a Sinkhole Region: A Study Toward Understanding Geohazards in the Karst Geosites

(Pencirian Geofizik di Kawasan Lohong: Suatu Kajian untuk Memahami Bahaya Geologi dalam Geotapak Karst)

SAWASDEE YORDKAYHUN*

ABSTRACT

The outstanding geosites in Satun UNESCO Global Geopark, Thailand are mainly karst topography. Sinkhole which is originated from the dissolution of karst rocks by groundwater or acidic rainwater is one of the potential natural disasters in these geosites. To gain the confident among geotourism, detecting karst features, cavities and surficial dissolution is crucial in risk assessment and sustainable geopark management. As a part of geohazard assessment, non-invasive geophysical methods were applied for detecting near-surface defects and karst features. In this study, electrical resistivity tomography (ERT), seismic tomography and multichannel analysis of surface waves (MASW) have been integrated to understand the mechanism of an existing sinkhole formation in Satun Geopark region. ERT appeared to be an effective approach to investigate the cavity development at shallow subsurface. MASW and seismic tomography were combined to help constrain the interpretation of lithology and karst features in vicinity of the sinkhole. The results indicated that the sinkhole occurrence in this area was probably developed by forming of cavity due to an increased dissolution of the fractured limestone bedrock. This carbonate layer is in contact with the overlying groundwater and weathering shale or cohesive soil layer. The changing of water table and infiltration of surface water by heavy rainfall allowed for a sudden vertical downward of overlying sediments into the empty voids, leading to the sinkhole hazard.

Keywords: Geosite; resistivity; Satun Geopark; seismic; sinkhole

ABSTRAK

Geotapak yang luar biasa di Satun UNESCO Global Geopark, Thailand adalah topografi karst. Kawasan lohong yang berasal daripada pembubaran batu karst oleh air bawah tanah atau air hujan berasid adalah salah satu potensi bencana alam di geotapak ini. Untuk mendapatkan keyakinan di kalangan pelancongan geografi, mengesan ciri karst, rongga dan pembubaran permukaan sangat penting dalam penilaian risiko dan kelestarian pengurusan taman geologi. Sebagai sebahagian daripada penilaian bahaya geologi, kaedah geofizik tidak invasif digunakan untuk mengesan kecacatan permukaan dekat dan ciri karst. Dalam kajian ini, tomografi kerintangan elektrik (ERT), tomografi seismik dan analisis pelbagai saluran ombak permukaan (MASW) telah disatukan untuk memahami mekanisme pembentukan kawasan lohong yang ada di wilayah taman geologi Saturn. Kelihatan ERT merupakan pendekatan yang berkesan untuk mengkaji perkembangan rongga di permukaan bawah yang cetek. MASW dan tomografi seismos digabungkan untuk membantu mengekang tafsiran litologi dan ciri karst di sekitar kawasan lohong. Hasil kajian menunjukkan bahawa kejadian lubang di kawasan ini mungkin dikembangkan dengan pembentukan rongga akibat peningkatan pelarutan batuan dasar batu kapur yang patah. Lapisan karbonat ini bersentuhan dengan air bawah tanah dan lapisan serpihan cuaca atau lapisan tanah yang bersatu. Perubahan meja air dan penyusupan air permukaan oleh hujan lebat memungkinkan mendapan mendadak ke bawah ruang kosong, yang membawa kepada bahaya kawasan lohong.

Kata kunci: Geotapak; kawasan lohong; kerintangan; seismos; taman geologi Saturn

INTRODUCTION

According to the UNESCO (2020), Global Geoparks are single, unified geographical area where sites and landscapes of international geographic significance are managed with a holistic concept of protection, education and sustainable development. In 2018, Satun Geopark has been promoted as a network of the UNESCO Global Geopark among the 147 Global Geoparks worldwide. It becomes the first

Global Geopark in Thailand and famous for the geotourism in Southeast Asia. Not only for geotourism, education, urban development and natural hazard management are also important issues to be fulfilled according to the terms and conditions for continuous promotion and certification as a Global Geopark. Like several karst-related Global Geoparks which are dominated in southern Europe and Southeast Asia (Ruban 2018), the main geological significances in Satun Geopark is karst topography. In such a geopark, landslide, rockfall, sinkhole, cave instability and subsidence constitute a serious hazard for human safety, infrastructures and land use in the geosites (Hellmy et al. 2019; Lai et al. 2018). Sinkhole is one of the geohazards that is developed by dissolution of karst rocks such as limestone, dolomite, anhydrite, gypsum, or salt by groundwater or water enriched with carbon dioxide (Watham et al. 2005). In Thailand, the northeastern, western and southern regions are reported by the Department of Mineral Resources (DMR) as the high risk of sinkhole due to the high abundance of soluble rock. However, mechanisms of sinkhole formations in these areas are site dependent by the difference in lithology, hydrogeology and trigger factors. For example, the sinkhole occurrence in northeastern Thailand is typically originated from rock salt (Satarugsa 2011), whereas limestone plays an important role in sinkhole occurrence in southern and western Thailand. Thus, detecting karst features such as cavities, surficial dissolution, calcareous bedrock and/or fractured zones are the key aspects to understand the sinkhole formation which is important in risk mitigation in the geopark.

As part of the sustainable geohazards management in Satun Geopark, geophysical investigation at a known sinkhole area is served as a preliminary study to assess the sinkhole hazard in the karst geosites. Therefore, the objectives of this work were to understand the mechanism of sinkhole formation using geophysical investigation and to propose a study plan for sinkhole hazard assessment in the geopark. A variety of geophysical methods, such as electrical resistivity tomography (ERT), ground penetrating radar (GPR), microgravity, seismic refraction and reflection methods have been successfully applied for sinkhole detection because of their potential to point out anomalies that may be associated with karst features (Beres et al. 2001; Carrière et al. 2013; Dobecki & Upchurch 2006; Kruse et al. 2006). Due to the complex landforms of karst terrains, the degrees of success are varied depending on the physical contrast between cavity and the surrounding rocks, their penetration depth and resolution (Martínez-Moreno et al. 2014). In this study, integrated ERT, seismic refraction tomography and multichannel analysis of surface waves (MASW) are used to detect the karst related features. Over the past two decades, a number of sinkhole and unstable karst system in Satun province has been reported by the Department of Mineral Resources (2013, 1997). Previous geophysical investigation in Satun province showed the depth of Ordovician limestone bedrock ranges from 0.5 to 35 m depth with an average depth of 20 m (Department of Mineral Resources 1997). For the existing sinkhole in this study, it occurred in an urban area about 20 km south of an important geosite of Satun Geopark. This phenomenon has caused concerns among the local people and become a serious threat to their properties. Thus, the results of this work are served as a guideline for the geoconservation and geohazard assessment in the karst geosites of Satun Geopark.

Materials and Methods

Site description

Satun UNESCO Global Geopark is located in the southern peninsula, Thailand approximately 970 km south of Bangkok. The geopark comprises both mainland and islands located in 4 districts of Satun province, occupying an area of around 2,600 km^2 (Figure 1). It is bounded on the west by the Andaman Sea and on the north and east by the north-south running mountain ranges. According to the significant geodiversity and biodiversity in Satun Geopark, at least 27 geosites are attractive places for the touring and learning activities (Sardsud & Wongwanich 2017). In particular, Satun area is well known as a fossil land because it is constituted by sedimentary siliciclastic, comprising sandstone, mudstone, shale, chert, and carbonate rocks where fossils and/or index fossils from complete periods of the Paleozoic Era are reported (Bunopas 1981; Wongwanich 1990). Moreover, it includes the outstanding topographic terrains such as Ordovician red Stromatolitic limestone and terrestrial karst which are widespread in about one third of the geopark area. These complex landforms make distinction of different geosites which lead to the diverse characteristic of each area, such as cave, waterfall, islands, and mountains (www.satun-geopark.com). There are two main karst-forming rocks in the geopark, including the Ordovician limestone (dark, thinly bedded) restricted to the south and east of area and the Permian limestone (pure, massive) mostly in the north and west. Triassic granites are exposed in the northeast of the Satun mainland and in the islands.

The area of geophysical surveys is located in Manung district which is a part of Satun Geopark mainland. As reported by the Department of Mineral Resources (2013), the high potential sinkhole area is in vicinity of the limestone mountain range in the north of the district. The most famous geosite in this region is the cave in the Ordovician limestone mountain of Thung song group, namely Phu Pha Phet cave (Figure 1). In October 27, 2017, there was a sinkhole occurrence in a temple, locating about 20 km south of the Phu Pha Phet

cave. A week after sinkhole occurrence, we conducted a field survey and geophysical investigation in the area. Field measurement found the sinkhole geometry having dimension of 20 cm in diameter (at the surface) and 22 m depth. According to Wattham et al. (2005), this is general characteristics of sinkhole occurrence in the alluvium, classifying as subsidence sinkhole. In case of relatively thick sedimentary cover, an alternative definition given by Cadarelli et al. (2014) is piping sinkhole. Locally, the study area lies in a flat terrain of Quaternary sediments which is mainly covered by unconsolidated surface materials of clay, silt and gravel. This zone is in contact with Silurian-Devonian unit of mudstone, sandstone, shale and quartzite. It is interesting to note that the shale has siliceous and carbonaceous textures and there were bedded limestone lens formed in this rock unit. Further north, Carboniferous-Permian unit of shale, sandstone, siltstone and chert is dominated. According to lithologies exposed in the core rock sample from available groundwater well located at 450 m south of the study area, the soft sediments is underlain by thick calcareous shale with different degree of weathering and compaction. It is interesting to note that there is evidence of deep carbonate rocks as indicated by existing calcite vein at 25-40 m depth (Table 1). Geochemistry data available in the groundwater well located in 2.4 km further south also supported evidence of carbonate rock as characterized by basic water (pH about 7.50) and high amount of hardness, TDS and bicarbonate (Table 2). However, geochemistry analysis of water samples from sinkhole indicated that surface water is slightly acidic water (Table 2). The water table fluctuation in this area is mainly influenced by two factors, hydraulic gradient and infiltration of surface water. Based on the two groundwater wells, the near site well showed remarkable groundwater table at 9 m depth and the drawdown up to 28 m depth, whereas the far site well at 2.4 km further south exhibited groundwater table at 3 m depth and the drawdown at 12 m depth. This indicated that the study area performed as a discharge area. For the draining of surface water, this area is affected by the two distinct monsoon seasons, rainy season in May to November and dry season in November to January.

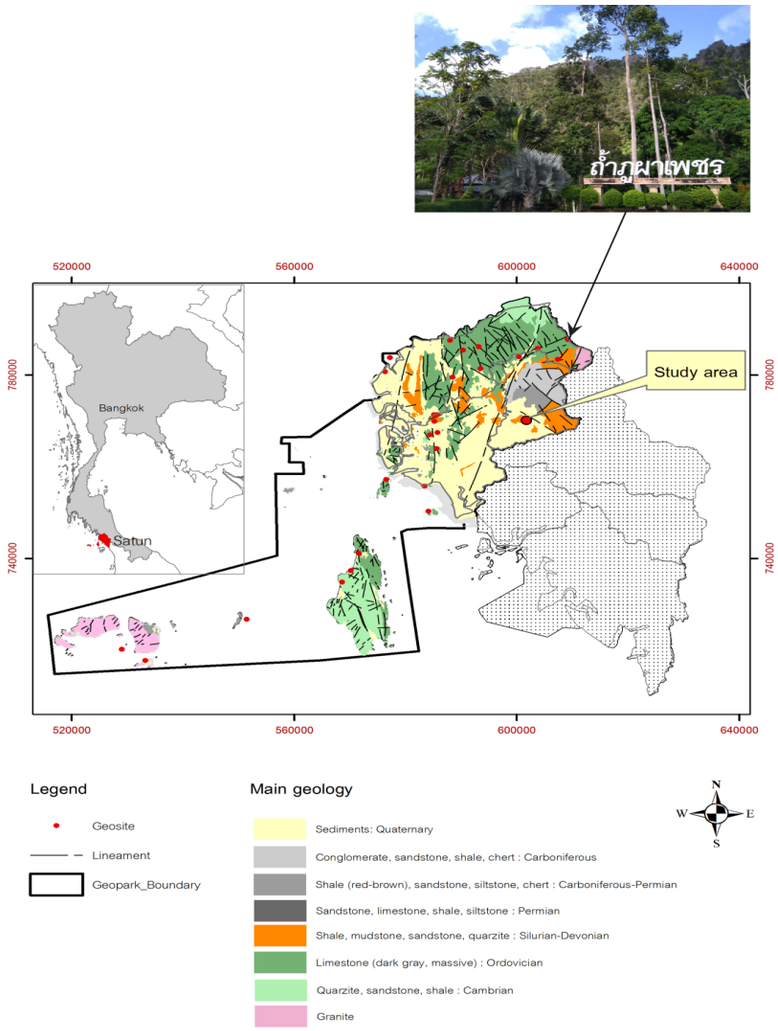

FIGURE 1. Geologic map of Satun geopark showing it's boundary and the study area

TABLE 1. Lithology information in the core rock samples from groundwater well (5512B020) located 450 m south of the sinkhole

Depth (m)	Lithology
0-6.0	Clay/gravel: Moderately reddish brown, granule around 40%, non-plastic, loose, composed of rock fragment
6.0-14.0	Shale: Medium gray, soft to stiff, slightly weathered, calcareous cemented, non-fissile
14.0-40.0	Shale: Grayish black, hard, slightly weathered to fresh, calcareous cemented, non-fissile, composed of calcite veins at 25.0-40.0 m

TABLE 2. Geochemistry analysis of water samples in the sinkhole and in the groundwater well located at 2.4 km south of study area

Item of analysis	Quantity	
	Sinkhole	Borehole (TM256)
pH	6.84	7.50
TDS	57 mg/L	158 mg/L
Hardness (as CaCO3)	33.6 mg/L	110.0 mg/L
Sulphate	5.0 mg/L	1.0 mg/L
Chloride	11.51 mg/L	12.0 mg/L
Sulfer	0.07 mg/L	-
Cu	0.02 mg/L	-
Zn	0.01 mg/L	-
Na	-	13.0 mg/L
Fe	1.61 mg/L	1.0 mg/L
Mg	-	6.1 mg/L
Bicarbonate	-	94.0 mg/L

GEOPHYSICAL METHODS

ERT

Concept of ERT permits the collection of vertical sounding and horizontal profiling simultaneously to generate a two-dimensional (2D) model of resistivity distribution in the subsurface using multielectrode system. Field measurement is conducted by injecting electric current through a pair of current electrode and measuring the potential different by a pair of potential electrode placed on the ground and controlled by switching device. The apparent electrical resistivity ρ_a beneath the subsurface at the middle points between the current and potential electrode over numerous stations can be calculated by (1).

$$\rho_a = k\frac{\Delta V}{I} \quad (1)$$

where I is the current and ΔV is potential different in the media. k denotes a geometric factor depending on electrode configuration.

ERT is one of the most suitable geophysical techniques applied in mapping karst features because the target is mainly regression zone formed as a result of voids or cavities in underlying strata. This zone can either be a high or low-resistivity anomaly, depending on the depth of groundwater table, dry and saturated condition in the area. Typically, deeper void space is characterized by the presence of low-resistivity features indicative of carbonate materials being replaced by looser clastic sediments, or by water. An air-filled void commonly generates a high-resistivity anomaly feature which is potential area of overlying sediments collapsed (Van Shoor 2002).

Knowing that karst system is highly variable laterally, dipole-dipole array is suitable when large data coverage as well as horizontal resolution is required (Zhou et al. 2002). In this study, a 120 m long of ERT survey line is run across the existing sinkhole using dipole-dipole configuration with 3 m electrode spacing. In this configuration, the electrode system is attached to a multicore cable in a straight line. The measurement is taken by four electrodes which are controlled by a computerized switching system of ABEM SAS1000 resistivity meter. For dipole-dipole arrays geometrical factor $k = n\pi(n+1)(n+2)a$. Where a is current electrode spacing which is equal to potential electrodes spacing. An integer multiple of a is referred to depth factor (n). The penetration depth was set in the range of n = 1-6, corresponding to surface down to about 17 m depth of investigation.

The raw data are processed using RES2DINV software (Loke 2003) to obtain inverted resistivity cross-sections. Data quality control is done as the first step by removing outlier apparent resistivity data to reduce geological noise which can be generated from several factors, such as shorting across the cable due to very wet ground conditions and very poor electrode-ground contact due to dry soil. In the inversion process, the subsurface is divided into a number of rectangular blocks and forward modeling routine is used to calculate the theoretical apparent resistivity pseudosection. Iterative inversion is performed by minimizing the difference between the calculated and measured apparent resistivity values by adjusting the resistivity of the model blocks until the root-mean squared (RMS) error is accepted and satisfactory convergence.

SEISMIC REFRACTION TOMOGRAPHY

The concept of seismic refraction method is based on sending seismic waves into the ground and recording the first arrival of seismic wave refracted from the different lithologies with elastic properties contrast, governing the Snell's law and Huygen's principle. In this method, a sequence of shot point and geophones placed on the ground allows for collecting and analysis of seismic traveltime versus distances. A number of techniques have been available to create 2D velocity model of the subsurface. The conventional layer model, such as intercept time method (Hagedoorn 1959), reciprocal or delay time method (Palmer 1980), work well in the case where the velocity distribution obeys the assumption of velocity increases with depth. In case of mapping karst features however seismic inversion and tomography method have proven to be suitable one for detecting low velocity zones (Yordkayhun et al. 2009).

In this study, four 70 m long seismic refraction survey lines were implemented across the existing sinkhole (Figure 2). Lines 1 and 2 are in north-south direction, while lines 3 and 4 are in west-east direction. To obtain the detailed images of sinkhole, both ERT and seismic surveys were integrated in line 2. A 24-channel Geometrics SmartSeis seismograph was used for data acquisition. Twenty four 14 Hz vertical component geophones were deployed at 3 m intervals. Shot points were located at 5 positions, including near and far offset on both ends and a middle of the line. The P-wave was generated by vertical hitting of 5 kg sledgehammer on a steel plate and vertical stacks (or hammer blows) were done at each shot point to enhance the signal to noise ratio. For all seismic profiles, the sampling interval was 0.5 ms, with a time window of 1024 ms. Although the refracted energy encountered within the first 100 ms (Figure 3), recording such a long time window is allowed for the MASW data analysis purposes.

To generate the P-wave velocity (Vp) model based on tomography methods, the first step was picking first arrival in the raw shot records. The traveltime versus offset data were used as input to generate an initial velocity model, representing the velocity distribution in the grid cells of subsurface. In a non-linear least squares inversion, the velocity model is updated iteratively to minimize the residuals between predicted traveltimes (forward model) and the observed traveltime until the acceptable model is obtained (Figure 3).

FIGURE 2. a) Geophysical survey lines, b) Sinkhole in the area, and c) Geophysical data acquisition

MASW

In fact, when seismic waves propagate in the inhomogeneous media, the surface waves exhibit the dispersion characteristic. This phenomenon can be observed in the shot record by the different slopes of high amplitude and low frequency waveform due to the different frequencies of surface wave have different phase velocities (Figure 3). The presence of surface wave is considered as noise for conventional seismic surveys. However, MASW method has taken this advantage by utilized phase velocity of surface wave to calculate the Vs profiles (Park et al. 1998). In an elastic medium, the propagation velocity of S-waves is given by.

$$Vs = \sqrt{\frac{\mu}{\rho}} \tag{2}$$

where μ is the shear modulus and ρ is the density of the media. Knowing the Vp and Vs, the geotechnical and earthquake engineering parameters related to geohazard assessment can be derived, such as shear modulus, Young modulus, Poisson's ratio, Vs30, and predominant site periods.

The detailed acquisition of active MASW data is described by Xia et al. (1999). In summary, MASW is likely to the conventional seismic reflection/refraction in terms of field procedure. However, field geometry and the low natural frequency geophone (~4.5 Hz) are the main parameters to consider for effective attenuation of background noise.

For MASW data processing, the first step was extracting the fundamental-mode dispersion curves using wavefield transformation of a shot gather from time-space (t-x) domain to phase velocity-frequency (f-v) domain. The dispersion curve was picked at the peaks of dispersion energy over different frequency values (Figure 3). Then, iterative least-squares inverse of dispersion curve was performed to generate 1-D Vs profile locating at the middle of the geophone spread by minimizing RMS error between the calculated and picked dispersion curve.

The main target of MASW in imaging karst features is the weak zone or presence of voids/cavities in underlying strata (Debeglia et al. 2006). The relatively weak nature of the sediments in this zone (low strength) is characterized by increased porosity compared to adjacent, undisturbed soil is a good contrast (velocity contrast) needed by MASW to give a better result. The zone is marked by reduced seismic velocities when imaged using the technique. Moreover, the Vs also used to determine the depth to top of bedrock and depression zones where highly stiff earth materials have relatively high Vs compared to fractured or weak earth materials (Olona et al. 2010).

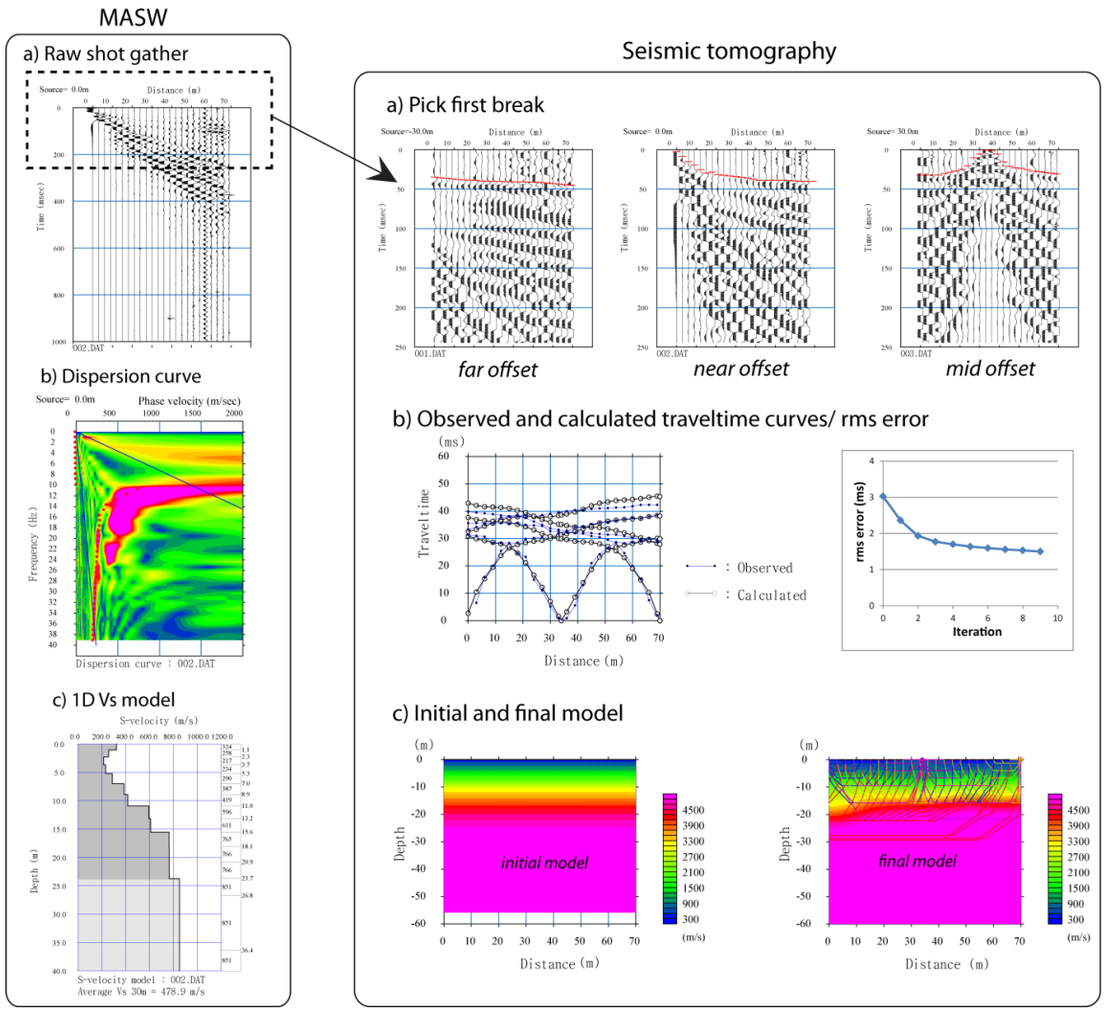

FIGURE 3. Seismic tomography processing, showing raw data with first arrival, traveltime curves and initial and final tomography model (right panel). MASW data processing, showing raw data, dispersion curve and inverted Vs model (left panel)

Results and Discussion

Lithology Interpretation

The resistivity section shows geologically complex structures over 16 m depth, whereas tomography section and Vs profile show the general trend of increasing Vp and Vs versus depth over 30 m depth (Figure 4). With constrained by an available groundwater well located about 450 m south of the study area (Table 1), four lithological layers can be distinguished within this depth range (Table 3).

First, the topmost 3 - 5 m thick unconsolidated sediment cover is characterized by low velocity, Vp of 400 - 1000 m/s and Vs of 100 - 300 m/s, respectively. The typical background resistivity values of this layer range from 100 - 1000 Ωm correspond to unconsolidated sediment of clay, sand and gravel with a slightly variable clay fraction. Decreasing of Vs at shallow depth (about 3m depth) indicates the present of saturated layer which agrees well with the recent water table visible in the sinkhole.

Second, the second layer with Vp of 1500 - 2000 m/s and Vs ranging from 400 to 600 m/s was found to be in good overall agreement with thick calcareous shale layer observed in the groundwater well. Within this layer, two regions of the low resistivity anomalies of < 100 Ωm were observed around the sinkhole. These zones can be interpreted as either clay or water-filled cavities since they exhibit similar conductivity parameters. However, on the basis of their shape, and resistivity values, the 8 - 15 m depth with round shape anomaly found in the north of sinkhole is likely to be water-filled cavity, whereas the shallow (3-8 m depth) and very low resistivity anomaly in the south of sinkhole is interpreted to be a clay lens.

Third, the third layer at a depth of 15 - 20 m (the deepest part of resistivity section) showed a high resistivity anomaly of > 1000 Ωm. Although intact limestone and air-filled cavity typically are characterized by high resistivity values (Van Schoor 2002), the high Vp of 2500 - 3000 m/s found within this depth suggested that this layer might be correlated with weathered limestone rather than air-filled cavity.

Fourth, the underlying half space layer showed a modulated morphology of the intact limestone bedrock, characterized by an average Vp and Vs of higher than 3000 and 800 m/s, respectively. There was a good correlation between the mapped depths to top of bedrock in seismic tomography section and 1D Vs profiles acquired along the same line (Figure 4). As stated earlier, the study area was in the contact zones of the two sedimentary units with different ages. Therefore, the limestone of this area is interpreted to be part of bedded limestone lens formed in the Silurian-Devonian rock unit.

TABLE 3. Summary of lithology and structural interpretation based on geophysical results

Lithology	Depth (m)	Resistivity (Ωm)	Vp (m/s)	Vs (m/s)
Unconsolidated sediments	0 - 5	5 - 100	400 - 1000	200 - 400
Calcareous shale/ weathered limestone	5 - 25	100 - 1000	1500 - 2000	400 - 700
Bedrock	15 - 25	> 1000	> 3000	> 700
Structures	Depth (m)	Resistivity (Ωm)	Vp (m/s)	Vs (m/s)
Water table	3 - 5	5 - 100	1500 - 1700	400 - 700
Cavities/clay	3 - 8 (clay)	5 - 100	NA	NA
	8 - 15 (water-filled)			
Fractures/faults	15 - 25	100 - 1000	Low Vp	Low Vs

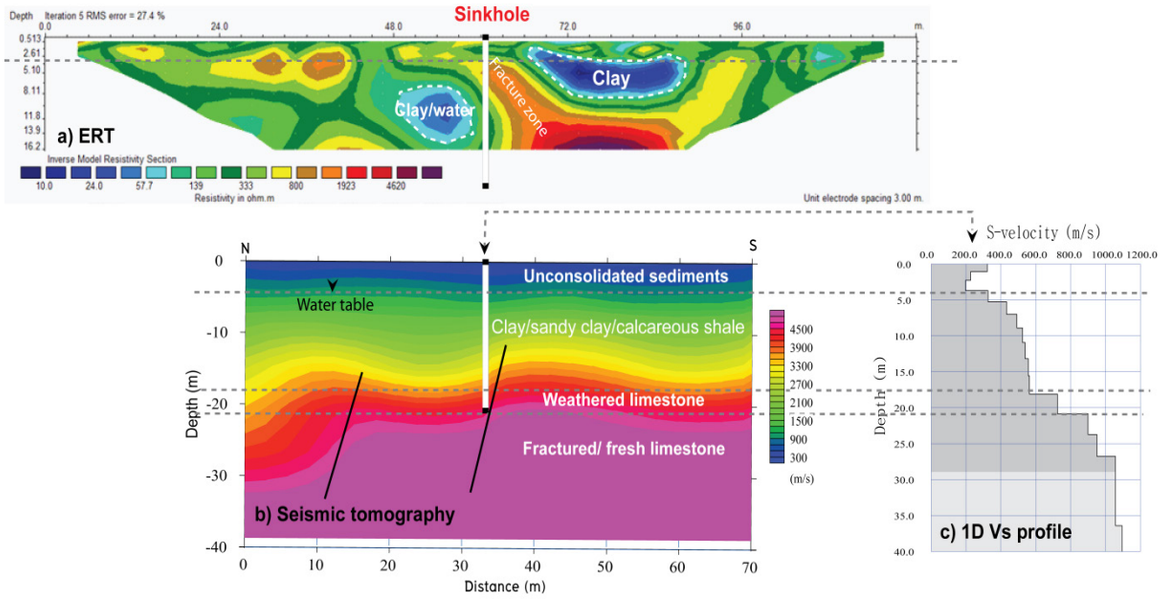

FIGURE 4. Correlation between ERT section, tomography section and Vs profile of line 2. Solid line marked the possible fractures

KARST FEATURES

Figure 5 displays the interpreted bedrock topography beneath the existing sinkhole along with Vp cross section, 1D Vs model, and Vp/Vs ratio at the middle of all seismic profiles. In combination with resistivity section, several key features of the geophysical results associated with the sinkhole and karst system were observed:

First, lateral discontinuities of resistivity exist down to depths of 5 - 15 m, indicating sub-vertical faults or fractures in the area (Figure 4). The clear evidence supporting subsurface movement can be seen on the presence of vertical offset of low-resistivity anomalies near the sinkhole. In resistivity section, this fracture zone is found at 3 - 10 m depth with approximately 4 - 6 m wide. It may be extended to the deeper subsurface as characterized by irregular bedrock topography (or pinnacles) in the tomography section. The presence of fractures enables pathways of water to seep down and reach the soluble bedrock. However, the deeper part of fractures in the bedrock was not detected in the tomography section due to the penetration depth limitation.

Second, the circular shape low-resistivity anomaly observed within a distance of 2 m from the sinkhole indicated evidence of soil decompaction. As mentioned before, it is subjective due to zones within the soil containing clay and fractures or cavity filled with water appear the same as low-resistivity anomaly zones (Abidin et al. 2017; Ezersky 2008). To provide insight into potential sinkhole formation, two scenarios may be considered. One possibility in case of soil containing clay and fracture, this anomaly might be formed by a sudden collapse of the clay lens along the fracture zone. In another case of water-filled cavity, it possibly formed by a cavity development through erosion process in the fracture zone. However, if this is the case, limestone bedrock is likely to expose at shallow depth or in the fracture zone. Consequently, we believe that cohesive soils (clay) and fractures play important role at shallow subsurface as evidenced from characteristics of existing sinkhole (very narrow, vertical piping).

Third, generally, seismic tomography distinguishes cavities, faults and fractures as zones with low Vp combined with low ray coverage (Yordkayhun et al. 2009).

In this study, the lateral resolution in the tomographic images may not resolve underground cavities due to the limited of shot points and ray coverage. However, it effectively outlined the variation of bedrock topography between 15 and 25 m depth. The top of bedrock is shallow in vicinity of sinkhole, indicating a possible formation of a high prominent set of solution-widened joints or fracture zone.

Fourth, the change in Vp of higher than 1500 m/s and increasing Vp/Vs ratio indicated water saturated layer below 5 m depth or high clayey silt content as mentioned by Signanini and Torrese (2004). By comparing this with water level observed in the local groundwater wells, sinkhole occurrence in this area could be associated with trigger conditions from local changing of water table and/or a sudden increase in surface water by heavy rainfall. However, the abrupt high Vp/Vs values that characterized depths below 15 m depth would be subjected to highly weathered and fractured layers.

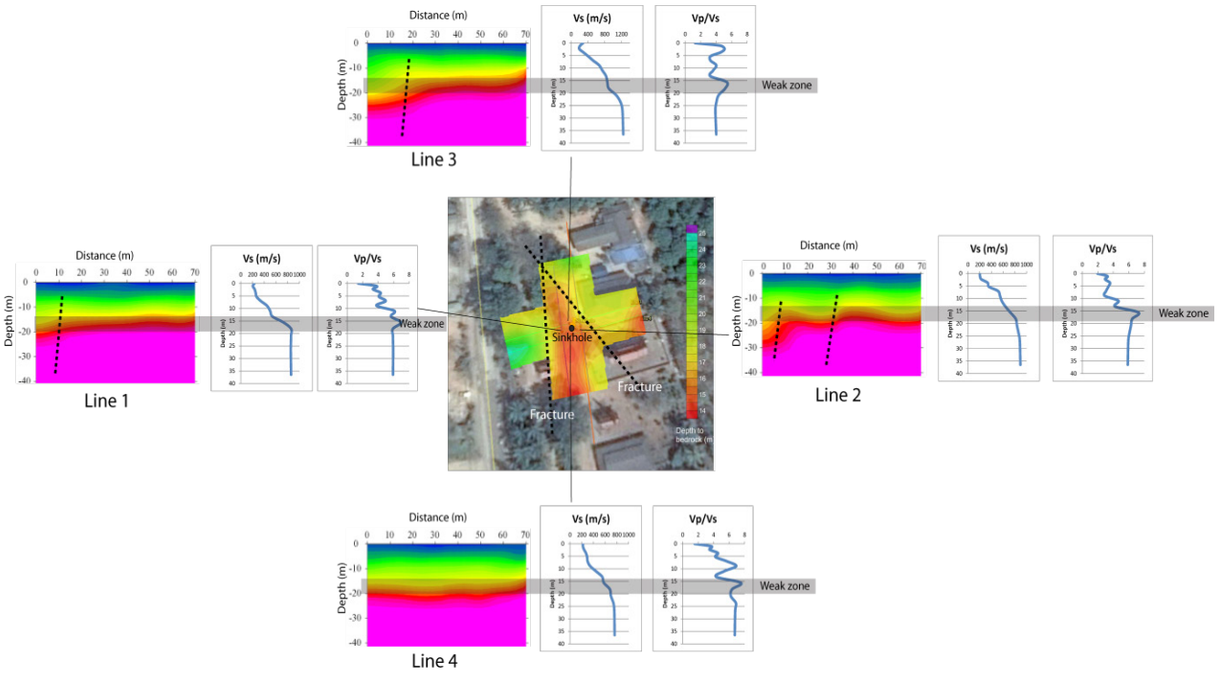

FIGURE 5. Bedrock topography map along with tomography sections, Vs and Vp/Vs of the 4 survey lines

THE MECHANISM OF SINKHOLE DEVELOPMENT

Based on the geophysical results, the sinkhole occurrence in the study area is a rapid clay-covered collapsed sinkhole in an area underlain by deep fractured carbonate bedrock. It's mechanism probably formed as the following stages (Figure 6).

First, acidic rainwater flows through the unconsolidated sediments infiltrated towards groundwater in the calcareous shale and/or clay-rich semiconfined layer and underlying fractured bedded limestone lens.

Second, dissolution enlarges the fractures, so that more water can flow into contact with deeper fractured

limestone and continues developing void or cavity. Dissolution generally made the fractures infilled with piped cohesive sediments of clays and silts.

Third, as a result of hydraulic pressure and gravity, the covering layer can disintegrate rapidly and falls down into the piped forming the pipe-like sinkhole. Declination of groundwater level and continue seeping down of surface water are also the trigger factors. It can be noticed that the observed shallow anomaly and mixed sediments nearby the sinkhole could be widened to some extent by gradual erosion process, resulting in a larger sinkhole and instability of the subsurface.

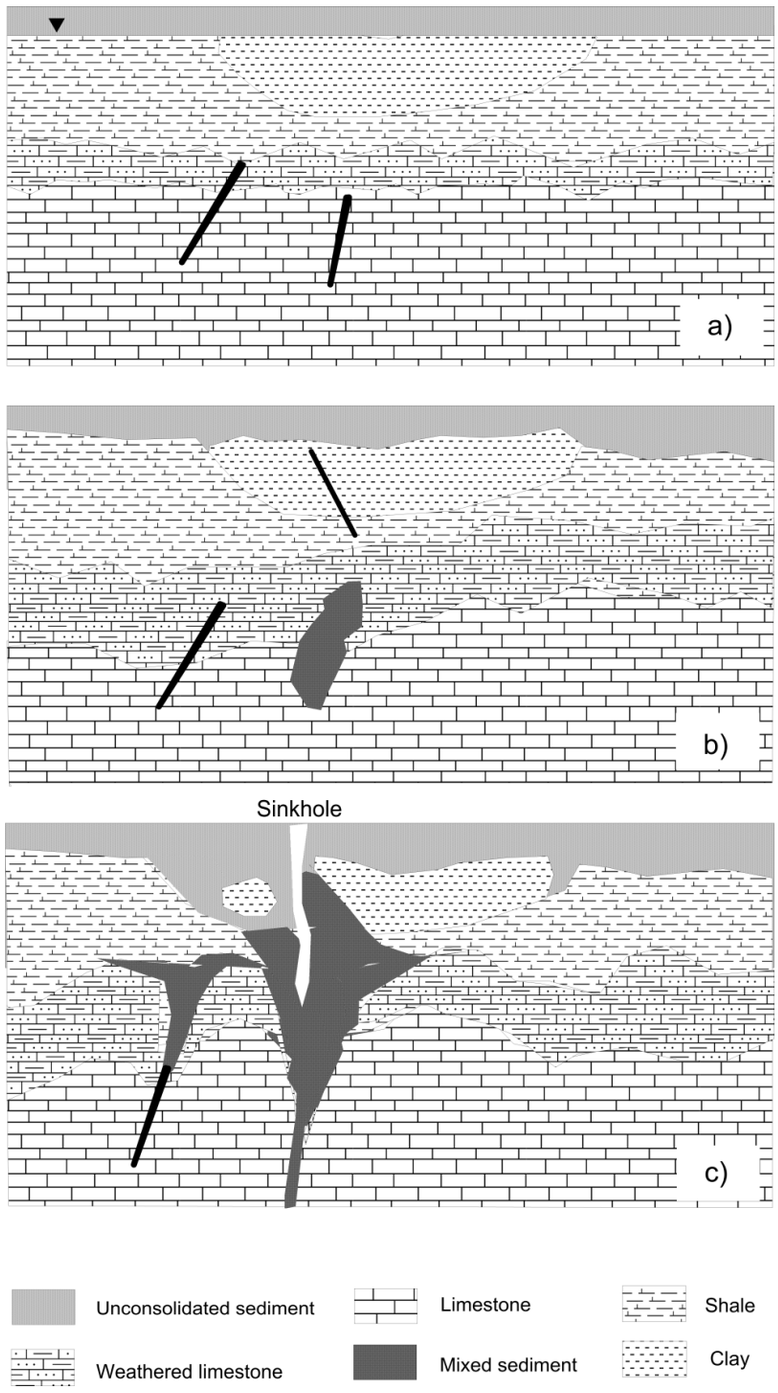

FIGURE 6. Schematic model of sinkhole formations in the study area (not to scale)

STUDY PLAN FOR SINKHOLE HAZARD ASSESSMENT

Lessons learnt from the case study provide a plan for sinkhole hazard assessment in the karst geosites of Satun Geopark. As summarized in Table 4, imaging subsurface in vicinity of sinkhole in the covered karst terrain is mainly emphasized on 3 components, lithology, geological structures, and hydrogeology. Knowledge on lithology, such as soil types and thickness of sediment covers and soluble bedrock contribute to the possible types of sinkhole and degree of weathering. Detecting void, fault and fracture zones is important in tracking the karstic recharge area or zones of enhanced dissolution. For hydrogeological studies, it may be desirable to determine whether a sinkhole formations and trigger as a natural or man-made groundwater decline. In this study, the geophysical results provided overall consistent images of karst system. However, indication of a broader fracture zone in limestone and depression zones are somewhat speculative in terms of depth and resolution. Consequently, the larger scale and integration of geophysical methods are suggested to implement in the geohazard assessment program. It should be noted that selection of appropriate geophysical methods is one of the critical factors in successful application because it is depended on the physical properties contrast between karst features and surrounding rock.

TABLE 4. Study plan for sinkhole hazard assessment in the karst geosites based on geophysical methods

Component of study	Karst related parameters	Potential geophysical methods	Outputs/Outcomes
Lithology	Sediment covers (soil type, texture and depth)	ERT, Seismic refraction, GPR, MASW	Degree of weathering Degree of saturation Cohesive/clastic/calcareous
	Bedrocks (rock type and depth)	Shallow: GPR, ERT, seismic refraction, MASW Deep: Seismic reflection, gravity, magnetic	Types of sinkhole Stiffness Degree of dissolution
Structures	Cavity/pipe (air-filled, water-filled)	Shallow: GPR, ERT, Electromagnetic (EM), seismic refraction, microgravity Deep: Seismic reflection, gravity, magnetic	Karst network
	Fracture/joint/fault	Shallow: GPR, ERT, EM, seismic refraction, MASW, microgravity Deep: Seismic reflection, gravity, magnetic	Karst network
Hydrogeology	Water table fluctuation (Natural and/or Man-made)	Shallow: GPR, ERT, EM, seismic refraction Deep: Resistivity sounding, Seismic reflection	Trigger condition Degree of saturation
	Ground water flow	GPR, ERT, seismic refraction, Seismic reflection	Recharge, discharge area
	Trace elements	Geochemistry	Acidic, basic or CO_2 rich-water

Conclusion

A preliminary study of geohazard assessment in the Satun UNESCO Global Geopark has been performed in the existing sinkhole area. Combination of resistivity and seismic methods permits the determination of a near-surface lithology based on the geoelectric and elastic properties of the subsurface. The ERT effectively imaged the possible shallow cavities and potential flow along the fracture of near-surface materials into karst at depth. Seismic velocity contrasts have confirmed the lithological structures and identified the depth of carbonate bedrock. The fractures or weathered zones of interaction between the bedrock and the overlying formations were highlighted by observed irregular bedrock surface. The sinkhole tends to form along the dominant fracture that control groundwater flow and draining of surface water. It appears that the cohesive soils and fractures play a crucial role in the pipe-like sinkhole in this area. Although this case study demonstrated an efficient mean of detecting sinkhole phenomena based on geophysical methods, understanding karst-related hazards in Satun Geopark is still challenging work. This is due to the difference in lithologies, structures, and hydrogeology conditions influences at different geosites make the karst system complicated and difficult to predict. Moreover, the geometry and structure of the karst system at deeper part were not clearly imaged due to the penetration and resolution limits of the methods. It would be suggested that the frontier larger scale geophysical surveys and hydrogeology information should be taken into account in the geohazards assessment program.

Acknowledgements

This work was supported by Prince of Songkla University (PSU) research grants, contract no. SCI6202054S. The author is grateful to the director of Satun UNESCO Global Geopark for the permission for field work. Department of Physics, Faculty of Science, PSU is thanked for supporting the field equipment and graduate students are thanked for their assistance during the field work. DMR is acknowledged for providing geology information.

References

Abidin, M.H.Z., Saad, R., Wijeyessekera, D.C., Ahmad, F., Baharuddin, M.F.T., Tajudin, S.A.A. & Madun, A. 2017. The influences of basic physical properties of clayey silt and silty sand on its laboratory electrical resistivity value in loose and dense conditions. *Sains Malaysiana* 46(10): 1959-1969.

Beres, M., Luetscher, M. & Olivier, R. 2001. Integration of ground-penetrating radar and microgravimetric methods to map shallow caves. *Journal of Applied Geophysics* 46(4): 249-262.

Bunopas, S. 1981. Paleogeographic history of Western Thailand and adjacent parts of Southeast Asia - A plate tectonics interpretation. Ph.D. thesis. New Zealand: Victoria University of Wellington. Reprinted in 1982 as Geological Survey Paper No.5. *Thailand: Geological Survey Division, Department of Mineral Resources*.

Carrière, S.D., Chalikakis, K., Sénéchal, G., Danquigny, C. & Emblanch, C. 2013. Combining electrical resistivity tomography and ground penetrating radar to study geological structuring of karst unsaturated zone. *Journal of Applied Geophysics* 94: 31-41.

Debeglia, N., Bitri, A. & Thierry, P. 2006. Karst investigations using microgravity and MASW; application to Orleans, France. *Journal of Near Surface Geophysics* 4(4): 215-225.

Department of Mineral Resources. 2013. *Geological Zoning for Geological Resources Management in Satun Province.* Bangkok: Department of Mineral Resources. p. 123.

Department of Mineral Resources. 1997. *Sinkhole Detection and Mitigation in Satun Province.* Songkhla: Mineral Resources Office. p. 57.

Dobecki, T.L. & Upchurch, S.B. 2006. Geophysical applications to detect sinkholes and ground subsidence. *The Leading Edge* 25(3): 336-341.

Ezersky, M. 2008. Geoelectric structure of the EinGedi sinkhole occurrence site at the Dead Sea shore in Israel. *Journal of Applied Geophysics* 64(3-4): 56-69.

Hagedoorn, J.G. 1959. The plus-minus method of interpreting seismic refraction sections. *Geophysical Prospecting* 7(2): 158-182.

Helly, M.A.A., Muhammad, R.F., Shuib, M.K., Fatt, N.T., Abdullah, W.H., Bakar, A.A. & Kugler, R. 2019. Rock slope stability analysis based on terrestrial LiDAR on karst hills in Kinta Valley Geopark, Perak, Peninsular Malaysia. *Sains Malaysiana* 48(11): 2595-2604.

Kruse, S., Grasmueck, M., Weiss, M. & Viggiano, D. 2006. Sinkhole structure imaging in covered karst terrain. *Geophysical Research Letters* 33(16): L16405.

Lai, G.H., Mang, W.J., Rafek, A.G., Serasa, A.S., Mazlan, N.A., Razib, A.M.M., Hussin, A., Ern, L.K. & Mohamed, T.R. 2018. Stability assessment of limestone cave: Batu Caves, Selangor, Malaysia. *Sains Malaysiana* 47(1): 59-66.

Loke, M.H. 2003. *Rapid 2D Resistivity & IP Inversion using the Least-Squares Method. Geotomo Software*. https://www.academia.edu/39226833/Rapid_2_D_Resistivity_and_IP_inversion_using_the_least_squares_method.

Martínez-Moreno, F.J., Galindo-Zaldívar, J., Pedrera, A., Teixido, T., Ruanoa, T., Peña, J.A., González-Castillo, L. Ruiz-Constán, A., López-Chicano, M. & Martín-Rosales, M. 2014. Integrated geophysical methods for studying the karst system of Gruta delas Maravillas (Aracena, Southwest Spain). *Journal of Applied Geophysics* 107: 149-162.

Olona, J., Pulgar, J.A., Viejo, G.F., Fernandez, C.L. & Cortina, J.M. 2010. Weathering variations in a granite massif and relted geotechnical properties through seismic and electrical resistivity methods. *Near Surface Geophysics* 8: 585-599.

Ortiz, D.G. & Crespo, T.M. 2012. Assessing the risk of subsidence of a sinkhole collapse using ground penetrating radar and electrical resistivity tomography. *Engineering Geology* 149(2): 1-12.

Palmer, D. 1980. The Generalized Reciprocal Method of Seismic Refraction Interpretation. *Australia: Society of Exploration Geophysics*. p. 104.

Park, C.B., Miller, R.D. & Xia, J. 1999. Multichannel analysis of surface waves MASW. *Geophysics* 64(3): 800-808.

Ruban, D.A. 2018. Karst as important resource for geopark-based tourism: Current state and biases. *Resources* 7(4): 82.

Sardsud, A. & Wongwanich, T. 2017. Role of geoheritage sites in contribution to development of Satun aspiring geopark. *DMR-CCOP-TNCU Technical Seminar on Biostratigraphy and Karst Morphology of Satun Aspiring Geopark.* pp. 50-59.

Satarugsa, P. 2011. The lessons learnt from geophysical investigation of sinkholes in rock salt in Thailand. I*nternational Conference on Geology, Geotechnology and Mineral Resources of Indochina* (GEOINDO 2011). pp. 445-455.

Signanini, P. & Torrese, P. 2004. Application of high resolution shear-wave seismic methods to a geotechnical problem. *Bulletin of Engineering Geology and the Environment* 63: 329-336.

Thepju, W., Yamansabedean, N. & Bamrungsong, P. 2017. Karst features in Satun geopark, Satun province. *DMR-CCOP-TNCU Technical Seminar on Biostratigraphy and Karst Morphology of Satun Aspiring Geopark. Thailand: Satun Aspiring Geopark*. pp. 50-59.

UNESCO. 2020. Global Geoparks. http://www.unesco.org/new/en/natural-sciences/environment/earth-sciences/unesco-global-geoparks/. Accessed on 11 March 2020.

Van Shoor, M. 2002. Detection of sinkholes using 2D electrical resistivity imaging. *Journal of Applied Geophysics* 50(4): 393-399.

Waltham, T., Bell, T. & Culshaw, M. 2005. *Sinkholes and Subsidence*. Berlin: Springer.

Wongwanich, T. 1990. Lithostratigraphy, sedimentology and digenesis of the Ordovician carbonates, Southern Thailand. University of Tasmania. Ph.D. Thesis. p. 215.

Xia, J., Miller, R.D. & Park, C.B. 1999. Estimation of near-surface shear wave velocity by inversion of Rayleigh waves. *Geophysics* 64(3): 691-700.

Yordkayhun, S., Tryggvason, A., Norden, B., Juhlin, C. & Bergman, B. 2009. 3D seismic traveltime tomography imaging of the shallow subsurface at the CO2SINK project site, Ketzin, Germany. *Geophysics* 74: G1-G15.

Zhou, W., Beck, B.F. & Adams, A.L. 2002. Effective electrode array in mapping karst hazards in electrical resistivity tomography. *Journal of Environmental Geology* 42: 922-928.

Division of Physical Science
Faculty of Science
Prince of Songkla University
Hat Yai, Songkhla, 90112
Thailand

Geophysics Research Center
Faculty of Science
Prince of Songkla University
Hat Yai, Songkhla, 90112
Thailand

*Corresponding author; email: sawasdee.y@psu.ac.th

Received: 16 March 2020
Accepted: 19 November 2020